ISSN 1069-3513, Izvestiya, Physics of the Solid Earth, 2011, Vol. 47, No. 6, pp. 475–487. © Pleiades Publishing, Ltd., 2011.
Original Russian Text © A.F. Grachev, D.M. Pechersky, V.A. Tsel'movich, 2011, published in Fizika Zemli, 2011, No. 6, pp. 13–25.

Titanomagnetites and Ilmenites from the Early Cenozoic Basalts and Limburgites of the Northern Tien Shan

A. F. Grachev[a], D. M. Pechersky[a], and V. A. Tsel'movich[b]

[a] *Schmidt Institute of Physics of the Earth, Russian Academy of Sciences, ul. Bol'shaya Gruzinskaya 10, Moscow, 123995 Russia*

[b] *Borok Geophysical Observatory, Schmidt Institute of Physics of the Earth, Russian Academy of Sciences, Borok, Yaroslavl Region, 152742 Russia*

Received October 13, 2010

Abstract—Based on X-ray spectrometry and thermomagnetic analysis, the chemical composition is studied and the Curie points are determined for the Early Cenozoic basalts and limburgites of the Northern Tien Shan. The microprobe analysis used in combination with the thermomagnetic analysis unambiguously identified a series of homogeneous primarily magmatic titanomagnetites in the studied samples against the broad variety of grains of titanomagnetite that underwent single-phase heterophase oxidation, which are often undetectable by a microprobe alone. The titanium content or TiO_2/FeO ratio in titanomagnetites and, correspondingly, the Curie points reflect the depth of the most recent equilibrium state of the magma, i.e., the depth of the magma sources. According to the dependence of the content of primarily magmatic titanomagnetite on the source depth, the latest equilibrium state of the magmatic melt of the Northern Tien Shan occurred at a depth of 40 ± 5 km. The obtained results agree with the reduction in the seismic velocities by a few percent below the Moho revealed by seismic tomography.

DOI: 10.1134/S106935131105003X

INTRODUCTION

Early Cenozoic volcanism in the Northern Tien Shan is an example of the evolution of the intraplate magmatism related with the emergence of the mantle plume approximately 55 Ma ago [Grachev, 1999; Gliko and Grachev, 1987]. In later works it has been shown that the plume extended as wide as to spread over the northwestern portion of China as well [Sobel and Arnaud, 2000], as inferred from the detailed geochemical analysis of basalts in that region [Grachev, 1999; Sobel and Arnaud, 2000] and from the results of seismic tomography [Vinnik, 1998].

In the past decade, plume magmatism was the subject of extensive research; however, the composition and the texture of the minerals such as titanomagnetites and ilmenites from the mantle plume rocks remained poorly studied. We believe that the study of the compositions of titanomagnetites and ilmenites from the magma plume rocks and their comparison with their counterparts from magma rocks of another origin will provide valuable additional information for diagnostics and better understanding of the plume magmatism from the stage of the magma storage in the upper mantle through the stage of magma crystallization.

Titanomagnetites and hemoilmenites are key magnetic minerals composing the magmatic rocks and, thus, the Earth's crust and the upper mantle. The particular compositional features of titanomagnetites and hemoilmenites, which primarily depend on temperature (T), redox conditions governed by the oxygen fugacity (fO_2), and general composition of a rock that undergoes crystallization, endow these minerals with genetic memory. Deciphering this memory provides a good insight into magma processes and the Earth's interiors overall [Genshaft et al., 1999; Pecherskii et al., 1975; Pecherskii and Didenko, 1995, etc.]. For example, the compositions of the concurrently crystallizing titanomagnetites and hemoilmenites are primarily governed by T-fO_2 conditions, and this fact lies behind the idea of the geothermometer and the Lindsley's fO_2 geobarometer [Spencer and Lindsley, 1981].

The Ti content in titanomagnetites is directly related to the depth of the magma chamber, or, more precisely, to the depth of the latest equilibrium state of magma before it rises to the surface and cools down, forming an intrusive body and/or outpours as lava [Pecherskii et al., 1975; Pecherskii and Didenko, 1995]. Ilmenite containing magnesium and chromium impurities is common in the plutonic rocks of the upper mantle and lower crust brought to the surface through eruptions of basaltic and kimberlitic magmas in the form of megacrysts. Such a magnesium variety of ilmenite (picroilmenite) can be used as a geobarometer. Similarly, the increased concentrations of chromium and aluminum in the titanomagnetite can indicate its plutonic origin.

In the present paper, we study the titanomagnetites and ilmenites from the Early Cenozoic volcanites of

the Northern Tien Shan. The targets of our research are rock samples acquired from the subvolcanic facies of the Uch-Kuduk neck (samples Ts90-5 and Ts90-6) and the Karakastek neck (samples Ts90-1, Ts90-1/3, and Ts90-2), those from the sill of the Boom Canyon (Baylamtal stow) (sample Ts90-3), and those from the lava flows in the Toraigyr River valley (samples Ts90-7/1, Ts90-7/2, Ts90-8/1, and Ts90-8/2). All the studied rocks have many features in common in terms of both the composition of the rock-forming minerals and the composition of the major, trace and rare earth elements, their increased maficity, and increased titanium content ($TiO_2 > 2\%$).

The first detailed description of one of the regions of the Uch-Kuduk neck was given by G.L. Dobretsov [Dobretsov et al., 1979], who identified the rocks forming this region as limburgites. The Karakastek neck is composed of massive analcite basalts with inclusions of plutonic ultrabasites and crustal rocks as well as megacrysts of olivine, clinopyroxene and spinel. The sill of the Boom Canyon and the Toraigyr lavas are composed of plagioclase-olivine basalts. Here, Fe-rich olivines are common, which reflects the shallow crystallization of the basalts. The Toraigyr basalts are considerably reworked, which resulted, in particular, in the increased silica content ($SiO_2 > 54\%$) and strong alteration of olivine after which iddingsite pseudomorphs develop [Grachev, 1999].

THE METHODS OF THE STUDY

The titanomagnetites and ilmenites were examined by X-ray spectrometry and thermomagnetic analysis. Compared to the other techniques, these two methods for studying the mineral composition of rocks have the significant advantage of providing *in situ retrieval of information* on the minerals contained in the rock sample (i.e., they do not require a specimen to be cut out from the rock mass).

X-ray spectrometry. The specimens were mounted in a washer 26 mm in diameter using the Wood alloy, then thoroughly ground, finely polished, and coated with a thin carbon film. The specimens were analyzed using the Camebax electron microprobe and Tescan scanning electron microscope (SEM) with an accelerating voltage of 20 KV and a beam current of 10 nA. The effective diameter of the probe was 2–3 μm, which was routinely monitored by the capture of a silica matrix containing fine grains of titanomagnetite. If a titanomagnetite grain measuring 3 μm gave no response in silica, this was regarded as indication of the probe diameter being below 3 μm.

We have studied the following parameters for the grains of titanomagnetite and ilmenite in the specimens: the grain size, the contents of FeO* (Fe content recalculated into FeO content), TiO_2, MgO, MnO, Cr_2O_3, and Al_2O_3. For each sample, up to 15 characteristic grains were analyzed. The Ni content was measured as well; however, we did not found any significant concentrations. The relative accuracy of determination of the mineral contents cited above was ±1%. Microphotographs were taken using the Tescan SEM in the electron backscatter mode.

Thermomagnetic Analysis. The thermomagnetic measurements were carried out using the Curie magnetic balance designed by Yu.K. Vinogradov. Due to its high sensitivity (the threshold percentage of detectability is 0.00001% content of magnetite and other magnetic minerals contained in a rock), the magnetic balance allows testing the magnetic minerals in specimens with a weight as small as 10–100 mg. The thermomagnetic analysis of a sample up to 700°C oC takes about 10 minutes. We analyzed the integral and the differential curves of temperature dependences for the induced magnetization of microsamples, i.e., carried out the thermomagnetic analysis (TMA) and the differential thermomagnetic analysis (DTMA). The TMA and DTMA curves for the first and the second heatings were then used for determining the Curies points of the magnetic minerals contained in a sample; for these minerals, we estimated their resistance to heating, which was treated as a diagnostic indicator of single-phase oxidation of titanomagnetite.

The Curie point is a fundamental characteristic of a magnetic material, which depends on its composition and on the structure of its crystalline lattice. In a series of solid solutions or in the magnetic minerals containing impurities that do not affect their crystalline texture, the Curie point is an unambiguous function of the mineral composition. TMA was conducted in a constant magnetic field with an intensity of 430 nT, which was knowingly the value of the magnetic saturation field for grains of titanomagnetite and ilmenite. According to the TMA curve, the contribution of each magnetic phase to the measured saturation magnetization was determined; the value of this contribution was divided by the value of saturation magnetization for the given mineral. The latter was estimated from the known composition–J_s-T_c dependence for titanomagnetites and ilmenites [Nagata, 1965]. Thus, we determined the approximate concentration of titanomagnetites and magnetite in each sample. Normally, the composition of the hemoilmenites in the studied collection corresponded to pure ilmenite with $T_c \approx -210$°C; even the hemoilmenite present in sample TS90-7/1 has $T_c \approx -100$°C. TMA was carried out at a temperature increasing from the room temperature; thus, ilmenites were beyond the temperature span of TMA and were not studied by TMA.

The TMA data (the measured Curie points) were compared with the compositions of grains measured by the microprobe (the estimated Curie points). For the samples containing grains of homogeneous titanomagnetite, the estimated and the measured Curie points should coincide. Their noticeable divergence indicates the heterogeneity of the magnetic mineral grains and, in particular, their breakdown, het-

erophase and single-phase oxidation, which are undetectable by microprobe due to the fine texture of the heterogeneity (below 0.02μm). Because no *detached* magnetite grains were found in any samples (see the table), the presence of magnetite and its allied minerals identified by TMA can be classified as a result of heterophase oxidation and the breakdown of titanomagnetites. Thus, the results of the microprobe and thermomagnetic analyses supplement each other.

THE RESULTS OF THE STUDY

The results of testing for each of 10 samples of the Northern Tien Shan volcanites can be briefly described as follows.

Sample Ts90-1 contains grains of homogenous titanomagnetite with a very uniform composition (table) and rather uniform shape and size (Fig. 1.) No impurities are found except for magnesium. The mean TiO_2 content is 17.4%, and the correspondent Curie point is 250°C. Taking into account the Mg impurity, the estimated Curie point is about 220°C. The measured Curie point is approximately 210°C (Fig. 2a). This means that the sample only contains primarily magmatic titanomagnetites. The concentration of titanomagnetite in the sample is about 5%. The second phase is close to magnetite (T_c = 570°C). Judging by the pattern of the TMA curve, magnetite is produced by the oxidation of titanomagnetite during laboratory heating (Fig. 2a).

Sample Ts90-1/3 contains grains of titanomagnetite that are uniform in composition (table) and homogenous. The sizes of grains and their almost uniform distribution in the rock (Fig.3a) are similar to those for sample Ts90-1. Almost isometric grains are predominant. Just as in sample Ts90-1, no impurities other than Mg are found. The average TiO_2 content is 18.7%, and the corresponding estimated Curie point is 215°C. The percentage of titanomagnetite in the sample is about 6%. The measured Curie point is 250°C (Fig. 2b); i.e., the titanomagnetite grains are oxidized (by single-phase oxidation). The microcracks that are visible in the titanomagnetite grains break them into blocks (Fig. 3b), which is typical for single-phase oxidation. The degree of single-phase oxidation is approximately 0.2, according to the Nishitani–Kono diagram [Nishitani and Kono, 1982]. The laboratory heating of titanomagnetite up to 700°C caused its heterophase oxidation, which increased its magnetization by a factor of 1.5 and changed its Curie point to 510°C.

Sample Ts90-2 contains grains of titanomagnetite and ilmenite and their intergrowths. Skeleton forms of the titanomagnetite grains are prevalent (Fig. 4a), which indicates that their crystallization occurred during the rapid cooling of lava. The grains of homogeneous titanomagnetite are very uniform in composition (table). The mean TiO_2 content is 14.5%, which corresponds to a Curie point of 310°C. The measured Curie point is570°C (Fig. 2c), which means that all

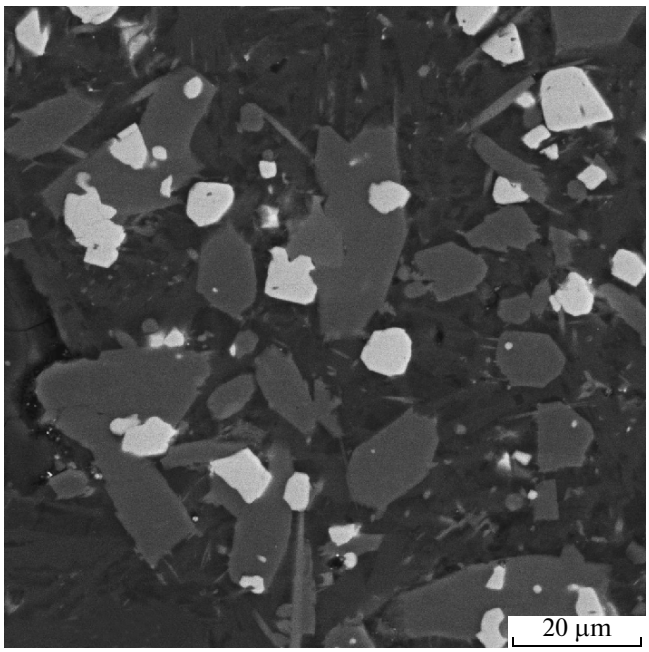

Fig. 1. Microscope images of grains of titanomagnetite in sample Ts90-1 (hereinafter, all images are obtained with the backscatter electron SEM mode). Grains of homogeneous titanomagnetite, general view.

grains of titanomagnetite are oxidized. A magnetic phase appears on the TMA curve at about 400°C (Fig. 2c). The heating completely eliminates this phase and reduces the magnetization to half the value, which indicates that this is the phase transition from maghemite to hematite rather than the Curie point. Therefore, the original titanomagnetite grains underwent heterophase oxidation to magnetite. Most often, the heterophase oxidation has a very fine texture, which is seen by the microprobe only in rare grains (Fig. 4b). A portion of magnetite, in turn, experienced single-phase oxidation (maghemization). The total content of magnetite and maghemite is about 5%. In contrast to samples Ts90-1 and Ts90-1/3, here, the titanomagnetite contains less Ti and practically does not contain any impurities (table). Separate grains of ilmenite contain manganese. According to the Lindsley geothermometer, the temperature of concurrent crystallization (if it was really the case) of the titanomagnetite and ilmenite intergrowths is approximately 550°C. This is, however, unlikely, because titanomagnetite in intergrowths has the same composition as its homogeneous grains. From this, it follows that the intergrowths are non-equilibrium, and ilmenite and titanomagnetite had crystallized in a different time and at a different T-fO_2.

Sample Ts90-3. Here, large grains of homogeneous ilmenite are definitely prevalent. The composition of the grains is rather uniform (table, Fig. 5a). Some grains are characterized by their increased manganese and aluminum content. The grains of ilmenite are

Mineral compositions of grains of titanomagnetite and ilmenite

Sample	TiO_2	FeO*	MgO	MnO	Cr_2O_3	Al_2O_3	CaO	SiO_2	Sum	T_c^*
Ts90-1, p. 1	17.3	77.2	1.8	0	0	0.2	0	0	96.5	
p. 2	17.0	77.9	2.0	0	0	0.2	0	0	97.1	
p. 3	17.1	77.3	1.6	0	0	0.2	0	0	96.2	
p. 4	18.1	78.2	3.4	0	0	0.2	0	0	99.9	
p. 5	17.9	77.3	3.0	0	0	0.2	0	0	98.4	
p. 6	17.2	77.9	1.8	0	0	0.1	0	0	97.0	
p. 7	17.3	77.8	1.6	0	0	0.2	0	0	96.9	
p. 8	17.3	76.9	1.8	0	0	0.2	0	0	96.2	
p. 9	17.4	77.5	2.6	0	0	0.2	0	0	97.7	
p. 10	17.4	76.9	2.0	0	0	0.1	0	0	96.4	
mean	17.4	77.5	2.2	0	0	0.16	0	0	97.2	250
Ts90-1/3, p. 1	18.4	77.0	3.0	0	0	0.3	0	0	98.7	
p. 2	18.5	76.8	3.0	0	0	0.2	0	0	98.5	
p. 3	19.1	75.7	3.0	0	0	0.2	0	0	98.0	
p. 4	18.6	78.8	2.8	0	0	0.4	0	0	97.8	
p. 5	19.2	76.3	2.6	0	0	0.1	0	0	98.2	
p. 6	18.8	76.0	2.8	0	0	0.1	0	0	97.7	
p. 7	18.5	76.8	3.0	0	0	0.2	0	0	98.5	
p. 8	18.6	76.3	2.7	0	0	0.3	0	0	97.9	
p. 9	18.6	75.9	2.8	0	0	0.2	0	0	97.5	
p. 10	19.0	76.3	2.8	0	0	0.1	0	0	98.2	
mean	18.7	76.5	2.85	0	0	0.22	0	0	98.0	215
Ts90-2 p. 1a	14.7	82.1	0.2	0	0	0.3	0	0	97.3	
p. 1a	45.0	53.9	1.0	0	0	0.2	0	0	100.1	
p. 2	14.0	80.9	0.3	0	0	0.1	0	0	95.3	
p. 3	14.3	80.8	0.3	0	0	0.1	0	0	95.3	
p. 4	14.5	81.3	0.2	0	0	0.1	0	0	96.1	
p. 5	15.0	81.0	0.1	0	0	0.1	0	0	96.2	
p. 6	14.1	81.7	0.1	0	0	0.1	0	0	96.0	
p. 7	14.2	81.3	0.1	0	0	0.1	0	0	95.6	
p. 8	45.5	50.9	1.2	2.9	0	0.1	0	0	100.6	
p. 9	15.0	81.1	0.1	0	0	0.2	0	0	96.4	
mean	14.5	81.3	0.2	0	0	0.14	0	0	96	310
Ts90-3, p. 1	50.2	48.0	0	0.1	0	0	0	0	98.3	
p. 2	50.3	48.1	0.1	0.1	0	0	0	0	98.6	
p. 3	50.4	46.9	0.1	2.3	0	2.0	0	0	101.7	
p. 4	50.0	45.1	0.1	0.8	0	6.0	0	0	102.0	
p. 5	50.2	45.2	0.0	2.6	0	3.0	0	0	101.0	
p. 6	50.7	46.9	0.1	0.6	0.1	0.3	0	0	98.7	
p. 7	50.1	45.9	0.1	2.3	0.1	2.2	0	0	100.7	
p. 8	50.9	46.2	0.1	0	0.1	0.7	0	0	98.0	
Ts90-5, p. 1	19.2	73.0	0	0.9	4.0	0.8	0	0	97.9	
p. 2	17.2	75.1	0.1	0.9	4.0	0.8	0	0	98.1	
p. 3	16.7	75.5	0.1	0.8	4.1	0.7	0	0	97.9	
p. 4	18.2	74.5	0	0.8	4.1	0.9	0	0	98.5	
p. 5	12.8	75.8	0.1	0.8	8.0	0.8	0	0	98.3	
p. 6	16.9	75.7	0.1	0.8	4.5	1.0	0	0	98.1	
p. 7	19.0	77.5	0.1	0.8	0.1	0.8	0	0	98.3	
p. 8	18.3	75.5	0.1	0.9	3.8	0.9	0	0	99.5	
p. 9	16.6	75.9	0.1	0.7	3.6	1.3	0	0	98.2	
p. 10a	49.1	44.5	5.1	0.8	0	0	0	0	99.5	
p. 10b	13.8	80.9	0.9	0.8	0	1.3	0	0	97.7	
mean	17.2	75.9	0.1	0.8	4.5	0.8	0	0	98.2	245

Table (Contd.)

Sample	TiO_2	FeO*	MgO	MnO	Cr_2O_3	Al_2O_3	CaO	SiO_2	Sum	T_c^*
Ts90-6, p. 1	18.2	73.8	2.4	1.2	0.5	1.2	0	0	97.3	
p. 2	17.5	76.1	2.4	1.1	0.3	0.9	0	0	98.3	
p. 3	20.8	73.1	3.3	1.1	0.1	0.8	0	0	99.2	
p. 4	19.2	75.1	3.2	0	0.1	0.8	0	0	98.1	
p. 5	21.3	72.4	3.4	1.0	0.2	0.9	0	0	99.4	
p. 6	17.7	76.1	2.5	0.8	0.1	0.8	0	0	98.0	
p. 7	20.5	73.1	3.0	0.9	0.4	0.8	0	0	98.7	
p. 8	20.8	72.9	2.9	0.9	0.3	0.8	0	0	98.6	
p. 9	18.8	74.1	3.0	0.9	0.2	0.8	0	0	97.8	
p. 10	17.2	76.6	3.1	0.8	0.1	0.9	0	0	98.7	
mean	19.2	74.3	2.88	0.95	0.18	0.8	0	0	98.7	205
Ts90-7/1, p. 1	30.2	63.5	0	1.9	0.2	3.6	0	0	99.4	
p. 2	18.1	79.3	0	0	0	0	0	1.3	98.7	
p. 3	17	79.8	0	0	0	0	0	1.2	98	
p. 4	18.5	75.5	1.3	0	0	0	0	4.7	100	
p. 5	16.2	75.4	1.9	0	0	0	0	6.5	100	
p. 6	11.4	84.2	0	0	0	0	0	4	96.6	
p. 7	13	83.9	0.6	0	0	0	0	1.2		
p. 8a	20.0	75.0	0	0	0	0	0	0	95.0	
p. 8b	38.7	50.6	0	1.0	0.2	0	0	0	90.5	
mean	18.1	77.1	0.5	0	0	0	0	2.4	98	220
p. 9	43.8	53.9	1.0	0	0	0	0	0.9	100	
p. 10	48.6	49.1	0.8	0	0	0	0	1.5	100	
p. 11	49.7	45.1	0	1.7	0.1	3.4	0	0	100.0	
p. 12	48.7	44.1	0	1.7	0.1	3.2	0	0	97.8	
p. 13	49.5	45.6	0	1.2	0.3	3.0	0	0	99.6	
p. 14	49.5	45.6	0	1.2	0.3	3.0	0	0	99.6	
p. 15	49.1	43.8	1.5	0	0	0	0	5.6	100	
p. 16	55.5	44.1	0.4	0	0	0	0	0.4	100	
p. 17	57.7	42.3	0	0	0	0	0	0	100	
p. 18	59	38.7	1.3	1.0	0	0	0	0	100	
p. 19	60.1	36.0	1.7	1.4	0	0	0	0.8	100	
p. 20	60.2	36.6	2.3	0.9	0	0	0	0	100	
p. 21	0	69.2	5.3	0	0	3.3	0.5	21.7	100	
p. 22	0	70.3	4.9	0	0	2.6	0.6	21.7	100	
p. 23	0	71.2	5.1	0	0	2.2	0.7	20.8	100	
p. 24	0	72.7	4.6	0	0	2.6	0	20.1	100	
p. 25	0	74.6	3.9	0	0	3.0	0	18.6	100	
p. 26	0	75.5	5.0	0	0	2	0	17.6	100	
p. 27	0	78.6	3.0	0	0	2.8	0	15.6	100	
p. 28	0	79.4	2.7	0	0	2.3	0.6	15.0	100	
p. 29	0	84.9	2.5	0	0	0	0	12.6	100	
p. 30	0	84.6	2.0	0	0	0	0	12.0	100	
p. 31	0	82.9	2.7	0	0	2.2	0.5	11.8	100	
p. 32	0	87	1.9	0	0	0	0.6	10.5	100	
Ts90-7/2, p. 1	3.7	74	2.0	0	0	3.8	1.1	14.9	100	
p. 2	2.8	71.3	2.4	0	0	3.5	1	17.8	100	
p. 3	3.6	73.1	2.4	0	0	3.6	1.1	15.8	100	
p. 4	2.7	72.2	3.1	0	0	3.9	1	16.6	100	
p. 5	5.1	74.3	2.0	0	0	3.3	0.9	13.5	100	

Table (Contd.)

Sample	TiO_2	FeO*	MgO	MnO	Cr_2O_3	Al_2O_3	CaO	SiO_2	Sum	T_c^*
Ts90-8/1, p. 1	47.1	50.5	1.0	0.4	0	0.1	0	0	98.1	
p. 2	29.9	68.5	0.8	0	0	0.1	0	0	99.3	
p. 3	27.9	65.5	0.9	0.3	0	2.3	0	0	96.9	
p. 4	53.8	45.0	2.0	0.8	0	0.1	0	0	101.7	
p. 5a	28.8	65.9	0.1	0	0	1.9	0	0	96.7	
p. 5b	56.8	42.0	0.3	0.9	0	0.1	0	0	100.1	
p. 6	27.0	67.9	1.0	0	0	2.1	0	0	97.8	
p. 7	26.9	68.8	1.1	0	0	1.8	0	0	98.6	
p. 8	28.8	67.9	1.1	0.4	0	0.5	0	0	98.7	
mean	28.2	67.4	0.83	0.1	0	1.5	0	0	98	50
Ts90-8/2, p. 1a	21.8	71.5	1.1	0	0.2	2.0	0	0	96.6	
p. 1b	51.0	44.5	2.1	0	0	0.6	0	0	98.2	
p. 2a	10.7	83.5	1.0	0	0	2.1	0	0	95.8	
p. 2b	44.7	53.1	2.1	0	0	0.7	0	0	100.6	
p. 2c, L.P.	17.7	75.9	2.1	0	0	1.9	0	0	97.6	240
p. 3a	44.8	52.3	2.5	0	0	0.8	0	0	100.4	
p. 3b	26.4	68.5	1.2	0	0	2.0	0	0	98.1	
p. 4a	45.5	51.0	2.8	0	0	0.8	0	0	100.1	
p. 4b	5.8	87.5	1.4	0	0	1.9	0	0	96.6	
p. 5a	46.1	51.3	2.7	0	0	0.6	0	0	100.7	
p. 5b	3.8	89.5	1.8	0	0	1.9	0	0	97.0	

Footnote 1: p.1, p.2, etc., are points (grains) of measurements with a microprobe; p.1a, p.1b, etc., denote measurements in the intergrowth of titanomagnetite and ilmenite. W.B. is the mean composition of the decomposed titanomagnetite is measured using the wide-beam microprobe; FeO* is iron content recalculated into FeO content; and T_c^* is the estimated Curie point calculated from the TiO_2 and TiO_2/FeO* contents in the grains of titanomagnetite. Mean denotes the mean composition of grains of titanomagnetite in the sample. Mean composition has not been calculated for samples Ts90-3 and Ts90-7/2 where grains of titanomagnetite have not been detected and for the sample Ts90-8/2 where most of the measurements have fallen either in the matrix or in the lamellae of the heterophasically oxidized titanomagnetites, sometimes with noticeable overlapping. T_c^* corresponds to the measurements with wide-beam

antiferrimagnetic, and their Curie point is about –210°C, that is, at room temperature and, especially at higher temperatures, they are non-magnetic. According to TMA, percentage of magnetite grains (T_c = 580°C, Fig. 2d) is 0.5%; according to microprobe analysis, these are very rare grains of titanomagnetite with evident structures of a breakdown (Fig. 5b), which is consistent with TMA.

Sample Ts90-5 contains a noticeable amount of grains of titanomagnetite (in forms close to the skeleton forms) and its intergrowths with ilmenite (Figs. 6a and 6b). The titanomagnetite grains are visibly homogeneous; the TiO_2 content in them slightly varies from 12.8% to 19% (table). The mean TiO_2 content is 17.2%, which corresponds to the estimated Curie point of 250°C. The measured Curie point is 260°C (Fig. 2e). Therefore, the grains are mostly homogeneous primary titanomagnetites; their content is about 3%. According to the Lindsley geothermometer, the intergrowths of titanomagnetite with ilmenite were formed at a temperature of about 550°C. Such an interpretation is favored, first, by the fact that the titanomagnetite from the intergrowth does not contain chromium, in contrast to other grains, which contain noticeable chromium impurities. Second, the Ti content is 3–5% lower than in the grains of homogeneous titanomagnetite. However, as seen from Figs. 6c and 6d, ilmenite had crystallized earlier than titanomagnetite. It is therefore more likely that ilmenites and titanomagnetites are minerals that belong to different generations and the Lindsley thermometer is inapplicable to them.

Sample Ts90-6. The grains of titanomagnetite are rather homogeneous (Fig. 7a), some with cracks that are typical for single-phase oxidation (Fig. 7b); titanomagnetite intergrowths with ilmenite occur. Similar to sample Ts90-5, the ilmenite in the intergrowths had crystallized earlier than the titanomagnetite. The latter contains considerable quantities of magnesium and minor manganese, chromium, and aluminum impurities. The TiO_2 content varies from 17.5% to 20.8% (table) about the mean value of 19.2%, which corresponds to the Curie point of 205°C. The TMA curve is a hyperbola in the interval from approximately 200 to 300°C (Fig. 2f), which indicates that there are homogeneous titanomagnetite grains with various compositions, from TiO_2 = 20% (T_c = 200°C) to TiO_2 = 15% (T_2 = 300°C). This is close to the scatter in the titano-

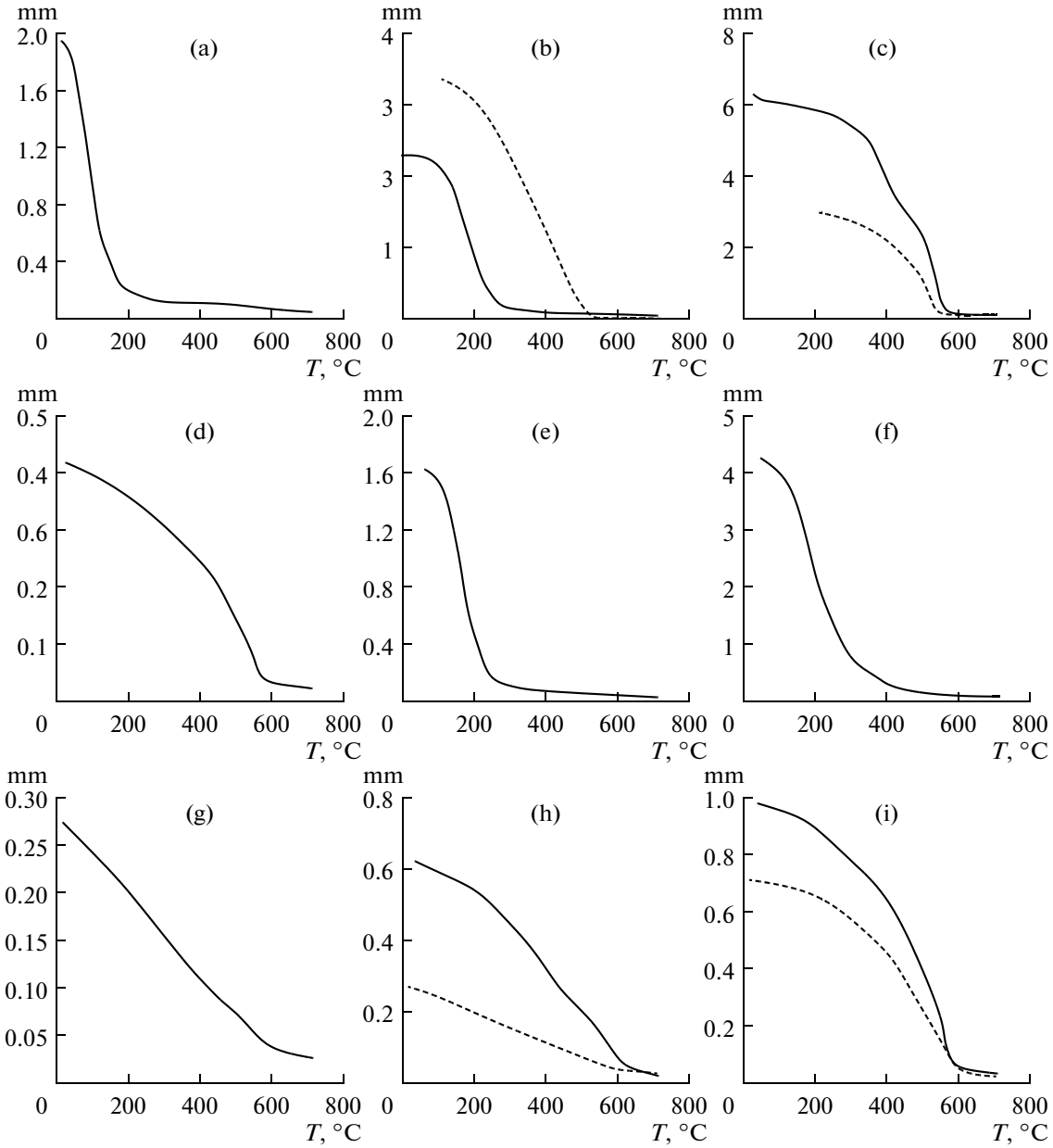

Fig. 2. Results of thermomagnetic analysis of basalt samples from the Northern Tien Shan.

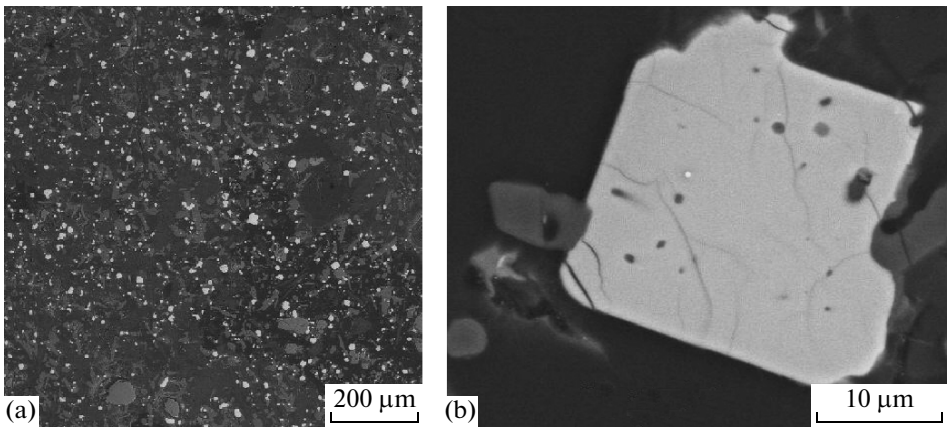

Fig. 3. Microscope images of grains of titanomagnetite in sample Ts90-1/3. Grains of homogeneous titanomagnetite: (a) general view; (b) grains of titanomagnetite with microcracks characteristic for the single-phase oxidation.

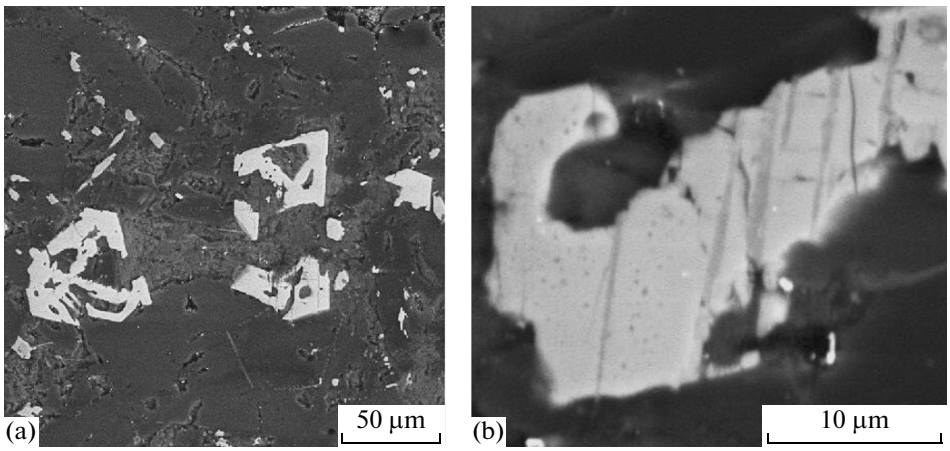

Fig. 4. Microscope immages of grains of titanomagnetite in sample Ts90-2: (*1*) skeletal grains of uniform homogeneous titanomagnetite; (*2*) heterophasically oxidized grain of titanomagnetite.

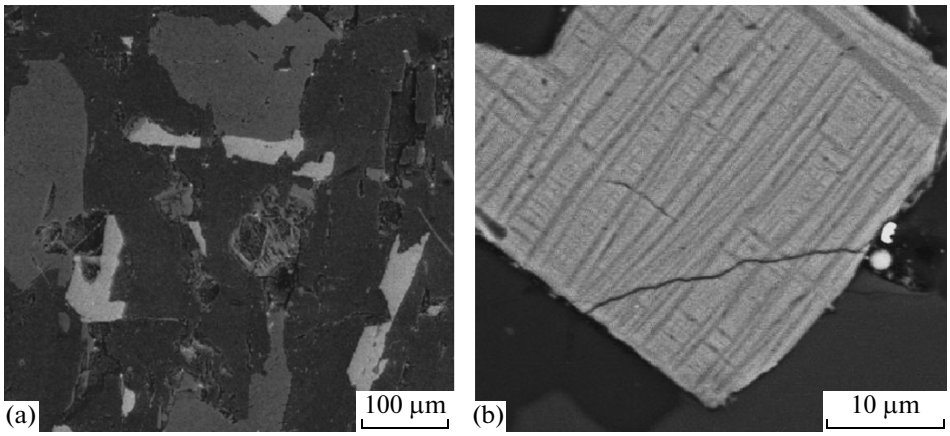

Fig. 5. Microscope images of grains of ilmenite and titanomagnetite in sample Ts90-3: (a) grains of ilmenite; (b) grain of heterophasically oxidized titnomagnetite.

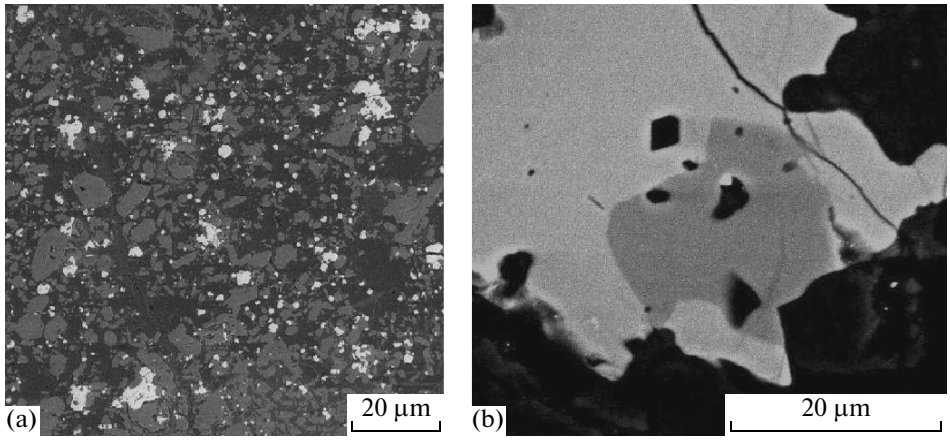

Fig. 6. Microscopem images of grains of titanomagnetite in sample Ts90-5: (a) general view; (b) intergrowths of titanomagnetite and ilmenite.

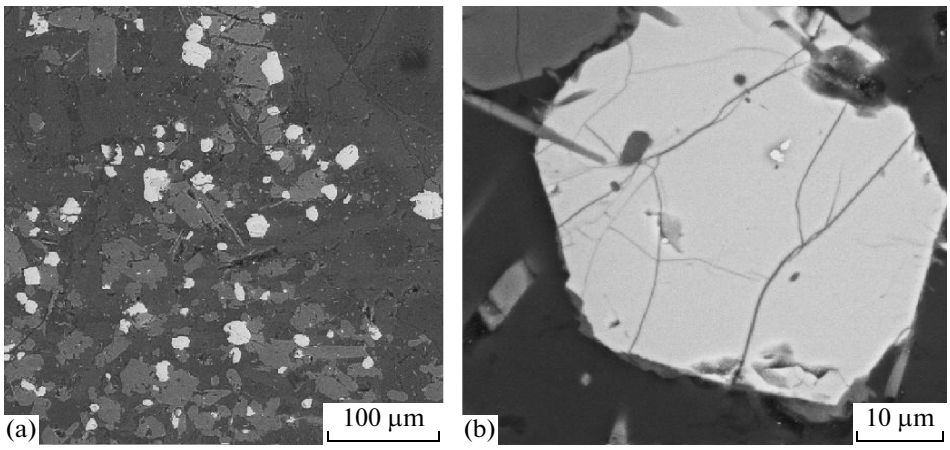

Fig. 7. Microscope images of grains of titanomagnetite in sample Ts90-6. Grains of titanomagnetite: (a) general view; (b) intergrowths of titanomagnetite and ilmenite with small cracks characteristic for single-phase oxidation.

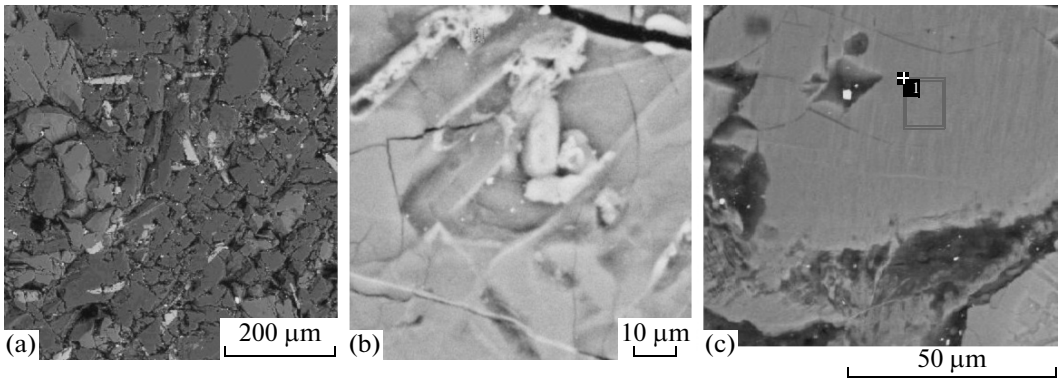

Fig. 8. Microscope images of grains of ilmenite and their intergrowths with titanomagnetite in sample Ts90-7/1: (a) general view, oblong grains of ilmenite are visible; (b) a fragment of a grain of ilmenite, fine grains of titanomagnetite are seen alongside them; (c) a grain of ferrous olivine (fayalite) pitted by iddingsite.

magnetite compositions yielded by the microprobe analysis (table). A part of grains probably underwent slight single-phase oxidation. $T_c \approx 500$°C is evidence of a single-phase and heterophase alteration of some titanomagnetite grains. The total concentration of titanomagnetite is approximately 10%.

Sample Ts90-7/1 is poorly polishable due to its loose structure. Rather large oblong grains of ilmenite (Fig. 8a) and, less frequently, fine grains of titanomagnetite 1–3 μm in size are identified. The latter are usually found in the small cracks of the ilmenite grains (Fig. 8b), that is, they are younger than ilmenites. Due to the small size of these grains of titanomagnetite, the microprobe beam "captured" the neighboring silicates, which resulted in the detection of 1–7% SiO_2 in them (table, sample 90-7/1, points 1–7). The mineral composition of fine titanomagnetite grains (table, sample 90-7/1, pp. 1–7) does not differ from that of the coarser grains of titanomagnetite in other samples. According to the Lindsley geothermometer, the crystallization temperature of a relatively large intergrowth of titanomagnetite and ilmenite (Fig. 8c, table, sample 90-7/1, pp. 8a and 8b) is about ~1100°C and fO_2 corresponds to Ni–NiO buffer, which is typical for the crystallization conditions of basalts. The mean TiO_2 content in the primarily magmatic titanomagnetites is 18.1%; the estimated Curie point is 220°C. The TMA curve exhibits a very slight show of $T_c = 210$°C close to the estimated T_c (Fig. 2g). The distinctly prevalent phase with $T_c = 590$°C (Fig. 2g), i.e., slightly oxidized magnetite, suggests that the grains of titanomagnetite likely underwent heterophase oxidation with very fine breakdown, which is invisible to a microprobe. The temperature of such oxidation and breakup should not exceed 400–500°C [Gapeev et al., 1986]. Another magnetic phase at about 400°C (Fig. 2g) is most likely the result of the transition of maghemite to hematite, which was observed in sample Ts90-2. The total titanomagnetite content is approximately 1%. Ilmenite contains manganese and aluminum impurities (table, sample 90-7/1, pp. 8–20). Frequently, the ilmenite grains are noticeably altered and cracked (Fig. 8b); at places, fine decomposition of ilmenite is visible. Alter-

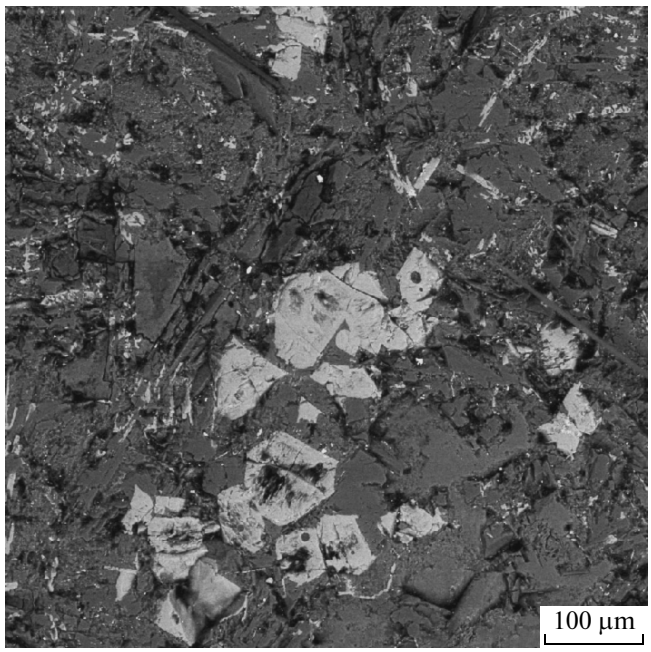

Fig. 9. Microscope images of grains of fayalite and ilmenite in sample Ts90-7/2.

ation of ilmenite increased the TiO_2 content in the ilmenite from 39% to 60%.

In samples 90-7/1 and 7/2, rather large phenocrysts of ferrous olivine are abundant (Figs. 8c and 9); their composition is close to fayalite (table, sample 90-7/1, pp. 21–32, and sample 90-7/2). The olivines are noticeably reworked; they contain fine lamellae, which reflect the secondary alteration of the fayalites to the iddingsites described previously in [Grachev, 1999]. The process of secondary alteration of olivine was accompanied by the reduction in the Si content and rise in the Fe content from 69% to 87% (table, sample 90-7/1, pp. 21–32). The latter is likely associated with the accumulation of iron oxyhydroxides (goethite) which is typical for iddingsite.

Sample Ts90-7/2 was very hard to polish due to its loose structure. The microprobe analysis revealed phenocrysts of ferrous olivine 50–100 μm in size and rare grains of ilmenite (Fig. 9) (for detailed description of sample Ts90-7/1, see table). As is evident from the TMA curve, the magnetic phase with $T_c = 620$°C is clearly predominant (Fig. 2h). It probably corresponds to the cation-deficient magnetite. The secondary magnetic phase near 400°C (Fig. 2h) reflects the transition of maghemite into hematite, which has been also observed for the other samples. The drop of magnetization by 35% after the first heating of the sample up to 700°C is due to the disappearance of maghemite and noticeable depletion of cation-deficient magnetite. After reheating, the Curie point becomes 580°C, and a small portion (~5%) of magnetization with the Curie point at approximately 610–620°C appears. The concentration of magnetite plus maghemite is approximately 0.5%.

Sample Ts90-8/1 contains titanomagnetite grains with the structures of the breakdown, which are typical for the high-temperature heterophase oxidation (Fig. 10a). The width of the lamellae of ilmenite is below 0.3 μm, which, according to the microstructural geothermometer, corresponds to the temperature of oxidation of at most 500°C [Gapeev et al., 1986]. Fine precipitates of rutile (Fig. 10b) that are indicative of the strong oxidation of titanomagnetite grains are distinguished under strong magnification inside the grains of the decomposed titanomagnetite. Skeleton forms of grains are predominant, which are due to the rapid crystallization of titanomagnetite at the stage of lava cooling. The titanomagnetite grains have rather similar mineral composition; the TiO_2 content varies from 27% to 30% (table), which corresponds to the estimated Curie point at 50°C. The measured Curie point $T_c = 600$°C (Fig. 2i) confirms heterophase oxida-

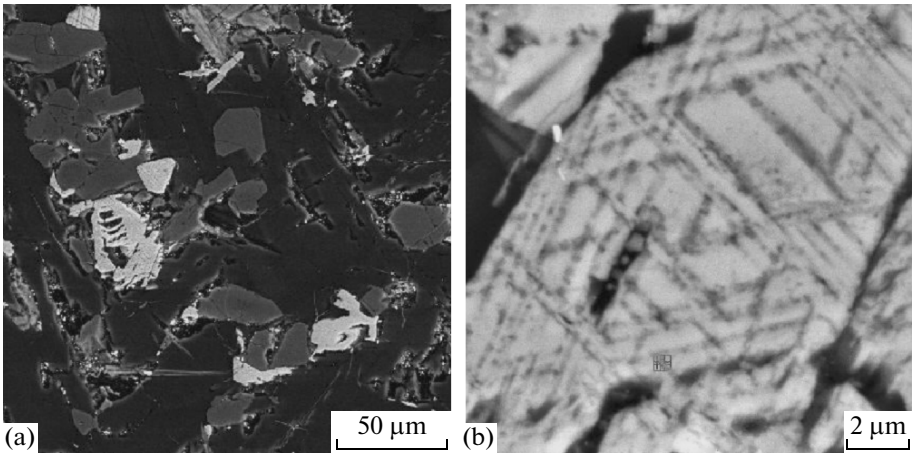

Fig. 10. Microscope images of grains of titanomagnetite in sample Ts90-8/1: (a) grains of titanomagnetite with a structure of high-temperature heterophase oxidation; (b) fine precipitates of rutile are visible inside the grains of decomposed titanomagnetite.

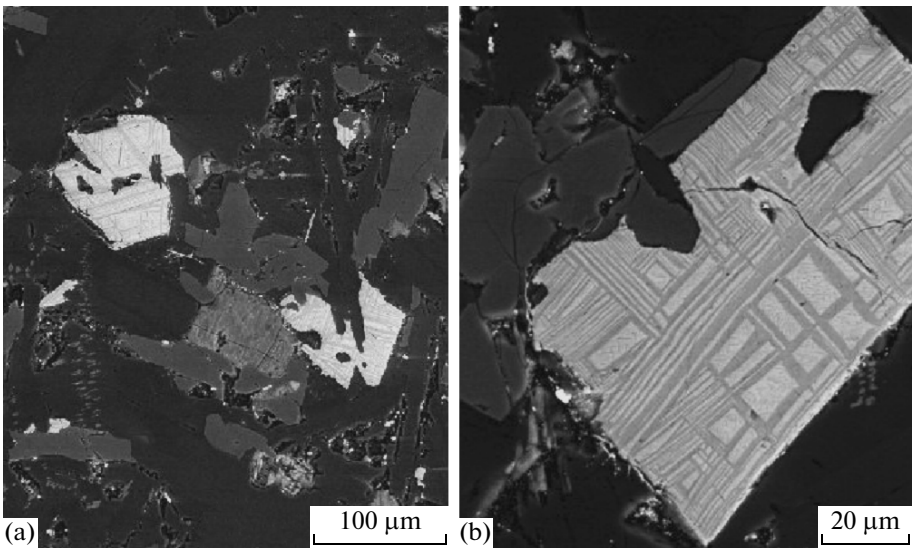

Fig. 11. Microscope images of grains of titanomagnetite in sample Ts90-8/1: (a), (b) grains of titanomagnetite with a structure of high-temperature heterophase oxidation.

tion of all titanomagnetite grains; this Curie point is preserved after the first heating up to 700°C. The concentration of magnetite is about 1%. Sample Ts90-8/1 contains fewer grains of titanomagnetite than the Ts90-1/3 sample. This is consistent with the value of the magnetic mineral content estimated from the magnetization: the difference is approximately fivefold. Minor concentrations of magnesium and aluminum are detected. The titanomagnetites of this sample feature high TiO_2 content, which distinguishes them against all other samples (table.)

Sample Ts90-8/2. Titanomagnetite grains with structures of breakdown, which are characteristic of high-temperature heterophase oxidation, are common (Figs. 11a and 11b). The lamellae of ilmenite are 1–3 μm in size, which corresponds to an oxidation temperature of about 1000°C, as estimated by microstructural thermometry [Gapeev et al., 1986]. According to the Lindsley geothermometer, the temperature of this breakdown ranges approximately from 900°C (points 2a and 2b, table) to750°C (points 4a, 4b and 5a, 5b, table). A finer imposed structure of relatively low-temperature breakdown is recognized inside the matrix of the high-temperature breakdown. The Lindsley geothermometer determines the temperature of the latest oxidation as at most 600°C. The TiO_2 content in the grain of titanomagnetite, measured by the large probe, is 17.7%, which corresponds to the estimated Curie point at 240°C, while the measured Curie point is T_c = 580°C. This corresponds to the high-temperature heterophase oxidation of all grains of titanomagnetite in the sample. In turn, inside the grains of the decomposed titanomagnetite, fine accumulations of rutile are apparent under strong magnification in both the matrix and the lamellae, which likely correspond to the deep multistage heterophase oxidation of the grains of titanomagnetite. Minor magnesium and aluminum impurities are recognized. The titanomagnetites of samples Ts90-8/1 and Ts90-8/2 considerably differ from all other samples in terms of the structure of the breakdown of the high-temperature heterophase oxidation. As well, some other shows of the rock alteration ($SiO_2 > 64\%$, considerably altered olivines) are characteristic of these two samples.

DISCUSSION OF THE RESULTS AND CONCLUSIONS

The study of the Early Cenozoic basalts and limburgites from the Northern Tien Shan revealed titanomagnetites and ilmenites in the samples examined. The concentrations of both the recognized minerals vary within rather wide limits; this follows from the measurements of the magnetization of samples: the percentage of titanomagnetite and magnetite, which is a product of the oxidation of titanomagnetite, range from a few fractions of a percent to 10%. The maximum concentrations of titanomagnetites are found in the limburgites from Uch-Kuduk, where they attain 10%. The Karakastek basalts are characterized by an almost similar percentage of titanomagnetites (5%); the basalts of Bailamtal and Toraigyr, in which nonmagnetic ilmenite is predominant, have the lowest concentration of titanomagnetites (at most 1%). A typical feature of the latter basalts is their noticeable secondary alteration, which, probably, resulted in the decomposition of most of the magnetic minerals. The basalts (for example, samples Ts90-2, 5, and 8) often contain skeleton forms of titanomagnetite crystals, which testify to their rapid crystallization in the cooling lava. The rapid crystallization is also responsible for the probable wide-range variations in the concen-

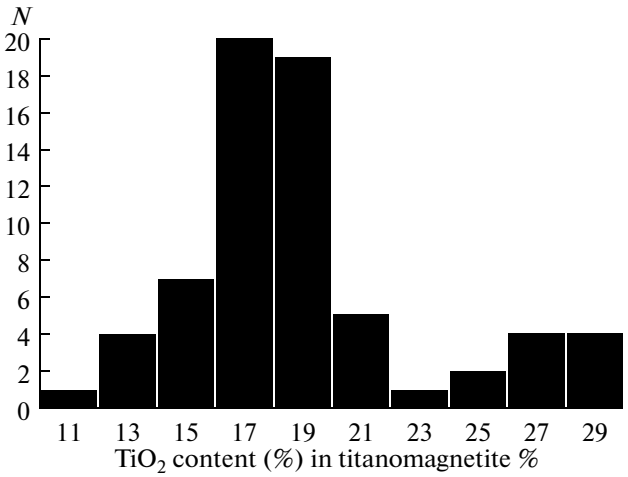

Fig. 12. Histogram of the titanium content (TiO_2,%) distribution in titanomagnetites.

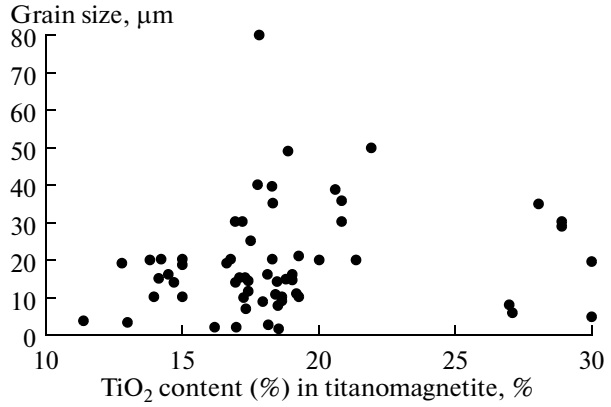

Fig. 13. Comparison of the titanium content (TiO_2,%) with the titanomagnetite grain sizes.

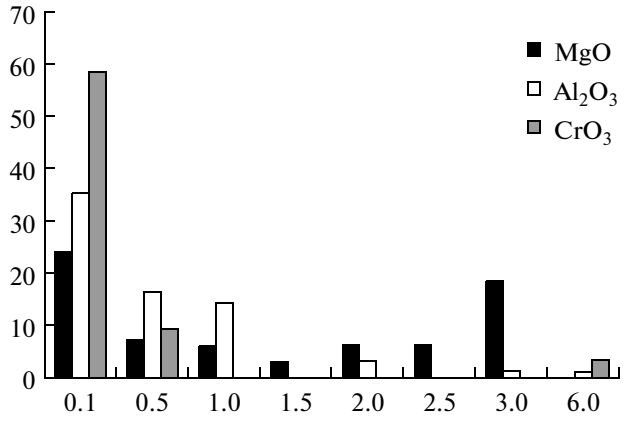

Fig. 14. Histogram of the aluminum, magnesium, and chromium content distribution in grains of titanomagnetite.

trations of the primarily magmatic titanomagnetite. Most frequently, the crystallization of grains of ilmenite had occurred before the crystallization of titanomagnetite, which can be seen from their relations in the limburgites of Uch-Kuduk; the concurrent crystallization of ilmenites and titanomagnetites is rarer. The basalts of Toraigyr (samples Ts90-7/1 and 2) contain phenocrysts of altered fayalite with the formation of iddingsite.

Combination of the microprobe and thermomagnetic analyses allowed us to unambiguously reveal a series of homogeneous primarily magmatic titanomagnetites in the examined samples against the broad variety of grains of titanomagnetite that underwent single-phase heterophase oxidation; homogeneous primarily magmatic titanomagnetites are often undetectable by the microprobe alone.

The composition of the primarily magmatic homogeneous and allied titanomagnetites is rather stable. It is clearly seen in Fig. 12 that most of the grains of titanomagnetite form a unitary set (in terms of TiO_2 concentration) with a distribution that is close to the normal distribution; the mean TiO_2 content is about 18%. The grains of titanomagnetite from sample Ts90-8/1, which form a separate set with a mean concentration of TiO_2 of 28%, are the only deviation from this set. We stress that this is a strictly local feature of the given sample: in the neighboring sample of Toraigyr rocks (Ts90-8/1), the TiO_2 content in the titanomagnetites is probably the same as in the other samples of the collection. The local pattern of this feature is highlighted by the fact that the distribution of the Ti-rich titanomagnetites is detached from the main group rather than linked to it by a smooth transition, which indicates that there are no titanomagnetites of intermediate compositions.

The Toraigyr basalts differ from the other samples in terms of Fe and Mg content, exhibiting a sharply higher iron content: FeO/(FeO + MgO) = 0.8, whereas in other rocks this ratio varies from 0.5 to 0.6 [Grachev, 1999], which is characteristic of the crystallization differentiation.

The Ti content practically lacks correlation with the size of the titanomagnetite grains (Fig. 13): the linear correlation coefficient r is 0.16. The almost constant Ti content in the bulk of titanomagnetites and the lack of its correlation with the grain sizes suggest that the thermodynamic conditions were stable both in the magma chamber and during the crystallization of titanomagnetite from the magmatic melt (in a system insulated from oxygen, the Ti content in titanomagnetites increases as magma crystallizes, from early generations to late generations; and, conversely, in an open system, the Ti content decreases from the early titanomagnetite generations to its late generations). This constancy is violated by the local crystallization differentiation of the individual extrusions of Toraigyr basalts. Constant Ti concentrations in titanomagnetites are typical for the rift basalts and unusual for the

island-arc volcanites. However, the TiO_2 content in the titanomagnetites of the rift basalts is normally 22–25%. Lower Ti content is characteristic of the titanomagnetites from the basalts of the intraplate plume magmatism [Pecherskii and Didenko, 1995].

Usually, aluminum, magnesium, manganese, and chromium are, if at all, present in minor concentrations in the grains of titanomagnetite and ilmenite, which is illustrated in Fig. 14. This indicates relatively late crystallization of these minerals during lava extrusion: by the time of crystallization of titanomagnetites, the melt had been already depleted in these minerals. The magnesium impurities, which are common in the titanomagnetites of basalts, are found in slightly higher concentrations attaining 3.5% in samples Ts90-1 and Ts90-6. Noticeable concentrations of chromium (up to 8%) are only recognized in the titanomagnetites of sample Ts90-5; that is, these titanomagnetites are likely of plutonic origin. However, the fact that the titanomagnetites had crystallized later than the ilmenites that do not contain any signs of deep crystallization (table) contradicts this interpretation. The studied rocks do not contain magnesium ilmenites of deep origin.

The titanium content or the TiO_2/FeO ratio in the titanomagnetites and, correspondingly, the Curie points reflect the depth of the latest equilibrium state of magma (that is, the depth of the magma source). According to the dependency of the mineral composition of primarily magmatic titanomagnetite on the magma source depth [Pecherskii et al., 1975; Pecherskii and Didenko, 1995], the depth of the latest equilibrium state of the magmatic melt in the Northern Tien Shan is 40 ± 5 km.

Our results agree with the reduction of a few-percent in the seismic velocities below the Moho revealed by seismic tomography [Kosarev et al., 1993; Vinnik, 1998].

REFERENCES

Vinnik, L.P., Seismic Properties of the Mantle Plumes, *Vestnik OGGGN RAN,* 1998, vol. 5, no.3, pp. 194–201.

Gapeev, A.K. and Tsel'movich, V.A., Microstructure of Natural Heterophasically Oxidized Titanomagnetites, *Izv. Akad. Nauk SSSR, Fiz. Zemli,* 1986, no. 4, pp. 100–104.

Genshaft, Yu. S., Tsel'movich, V.A., Gapeev, A.K., Solodovnikov, G.M., Value of Fe-Ti-oxide Minerals in the Earth's Science, *Vestnik OGGGN RAN,* 1999, vol. 1, no. 7, pp. 3–12.

Gliko, A.O. and Grachev, A.F., On the Nature of Deep Processes Responsible for Evolution of Regions of Intraplate Magmatism and Continental Rifts, *Dokl. Akad. Nauk SSSR,* 1987, vol. 295, pp. 64–67.

Grachev, A.F., Early Cenozoic Magmatism and Geodynamics of North Tien Shan, *Fiz. Zemli,* 1999, no. 10, pp. 26–51 [Izv. Phys. Earth (Engl. Transl.), 1999, vol. 35, no. 10, pp.?815–839].

Dobretsov, G.L., Kepezhinskas, V.V., Knauf, V.V., and Usova, L.V., Ultramafic Inclusions in Limburgites of the Northern Tien Shan and the Problem of Pyroxenites in the Upper Mantle, *Geol. Geofiz.,* 1979, no.3, pp. 65–77.

Nagata, T., *Rock Magnetism,* Tokyo: Maruzen, 1961.

Pecherskii, D.M., Bagin, V.I., Brodskaya, S. Yu., and Sharonova, Z.V., *Magnetizm i usloviya obrazovaniya izverzhennykh gornykh porod* (Magnetism and Conditions of Formation of Igneous Rocks), Petrova, G.N., Ed., Moscow: Nauka, 1975.

Pecherskii, D. M., and Didenko, A.N., *Paleoaziatskii okean* (Paleo-Asian Ocean), Moscow: OIFZ RAN, 1995.

Kosarev, G.L., Petersen, N.V., Vinnik, L.P., and Roecker, S.W., Receiver Functions for the Tien Shan Analog Broadband Network: Contrasts in the Evolution of Structures across the Talasso-Fergana Fault, *J. Geophys. Res.,* 1993, vol. 98, pp. 4437–4448.

Nishitani, T. and Kono, M., Grain Size Effect on the Low-Temperature Oxidation of Titanomagnetite, *J. Geophys. Res.,* 1992, vol. 50, pp. 137–142.

Spencer, K.J. and Lindsley, D.H., Solution Model for Coexisting Iron-Titanium Oxides, *Amer. Mineralogist,* 1981, vol. 66, pp. 1189–1201.

Sobel, E.R. and Arnaud, N., Cretaceous–Paleogene Basaltic Rocks of the Tuyon Basin, NW China and the Kyrgyz Tian Shan: the Trace of a Small Plume, *Lithos,* 2000, vol. 50, pp. 191–215.